Preprints.org

Article

Development of Innovative Composite Nanofiber: Enhancing Polyamide-6 with ε-Poly-L-lysine for Medical and Protective Textiles

Saloni Purandare , Rui Li , Chunhui Xiang [*] , Guowen Song [*]

Article

Development of Innovative Composite Nanofiber: Enhancing Polyamide-6 with ε-Poly-L-lysine for Medical and Protective Textiles

Saloni Purandare, Rui Li, Chunhui Zhang * and Guowen Song *

Iowa State University of Science and Technology
* Correspondence: chxiang@iastate.edu (C.Z.); gwsong@iastate.edu (G.S.)

Abstract: A novel electrospun nanofiber was developed using polyamide-6 (PA) and ε-poly-L-lysine (PL). PA is a popular textile polymer having desirable mechanical and thermal properties, chemical stability, and biocompatibility. However, PA nanofibers are prone to bacterial growth and user discomfort. PL, a natural homopolyamide, is non-toxic, antimicrobial, and hydrophilic but lacks spinnability due to its low molecular weight. Given its similar backbone structure as PA, with an additional amino side chain, PL was integrated with PA to develop multifunctional nanofibers. This study explores a simple, scalable method to obtain PL nanofibers by utilizing the structurally similar PA as the base. The goal was to enhance the functionality of PA by addressing its drawbacks. The study demonstrates spinnability of varying concentrations of PL with base PA while exploring compositions with higher PL concentrations than previously reported. Electrospinning parameters were studied to optimize the nanofiber properties. The effects of PL addition on morphology, hydrophilicity, thermal stability, mechanical performance, and long-term antimicrobial activity of nanofibers were evaluated. The inclusion of PL in PA-based nanofibers resulted in super hydrophilicity, increased tensile strength, and efficient antimicrobial properties with long-term stability. These enhanced characteristics hold promise for the composite nanofiber's application in medical and protective textiles.

Keywords: ε-poly-L-lysine; polyamide; antimicrobial textiles; hydrophilic; nanofiber

1. Introduction

Nanofibers are fibers with a diameter less than 1000nm. Nanofibers are gaining increasing attention due to advantageous characteristics such as high surface-to-volume ratio, low-pressure drop, good interconnectivity of voids, and controllable connectivity and morphology. Nanofibers find applications in a wide range of areas owing to their advantages, particularly in medical and protective textiles [1]. Electrospinning is a commonly used method to spin nanofibers wherein a viscoelastic spinning solution is fed at a continuous rate through a needle, and the needle is supplied with high voltage. The electrostatic forces overcome the surface tension of the drop at needle tip to form a jet. The jet stretches and solidifies into nanofiber on its way to a grounded collector [2]. The popular use of the electrospinning technique is mainly due to its simple, cost-effective setup and ability to manipulate the surface features and morphology of nanofibers [3,4].

Functional textile is a category of textile products, specially engineered for a predetermined functionality above body covering and aesthetics. The vast area of functional textiles includes several categories, such as but not limited to protective, medical, sports, and electronic textiles[5]. Functional textile research has established several innovative solutions that enhance the quality of life of the user. However, optimization of functional textiles is an on-going journey with challenges in capturing real use scenario along with factors such as the scalability, durability, reusability, and non-toxicity of the textile [6]. One of the category of functional textiles is antimicrobial textiles. The antibiotic resistance of bacterial strains and unavoidable bacterial contamination despite rigorous hygiene protocols calls for antimicrobial surfaces in medical and protective settings [7,8]. Antimicrobial function in textiles prevents microorganisms from reaching the wearer and vice versa; therefore, it remains essential for a healthy environment, especially in a medical setting. The antimicrobial function also allows for the

material to be self-decontaminating, ensuring the textiles' usability throughout its shelf time [9,10]. Leaching and synthetic antimicrobial agents exhibit toxicity towards wearer, therefore, highlighting the importance of naturally occurring non-toxic antimicrobial agents [10,11].

ε-poly-L-lysine (PL) is a cationic homopolyamide naturally produced by the filamentous bacterium Streptomyces albulus [12,13]. The naturally occurring homopolyamide has antimicrobial function owing to the cationic α-amino group. PL has been found to exhibit antimicrobial function through the destruction of microbial growth via electrostatic adsorption towards a wide range of Gram-positive and Gram-negative bacteria [12–14]. Either naturally or bio-synthetically, PL is commonly available at low molecular weights. The available low molecular weight (3600–4300 Da) has been established for effective antimicrobial function due to the presence of 25-30 L-lysine residues exhibiting cationic action against microorganisms. However, the low molecular weight limits spinnability of PL into a material [12,14,15]. Thus, nanocomposite of PL only in small concentrations with carrier polymers such as chitosan [16,17]; gelatin [18,19]; and poly(hydroxybutyrate) [20] is being increasingly explored for a wide range of applications such as food preservation, food packaging, wound dressing, and drug carrier. Studies have exhibited improved bactericidal effect with increased bacterial damage upon increasing the concentration of PL [19,21]. Results of several analyzed literature also supports improved antibacterial properties with increased PL concentration [16,17,22]. Further, cationic polymers such as PL experience proliferation of bacteria on the surface once the surface is sufficiently covered with microorganisms due to the exhaustion of cations [7,23,24]. A fiber system with an increased percentage of active antimicrobial sites can be expected to have efficient and stable contact-induced antimicrobial function. Along with improved antimicrobial efficiency, studies have also shown improved hydrophilicity with increased PL concentration [16,17,19]. Therefore, there is an existing gap in researching a fiber system with a high concentration of PL, possibly by copolymerization or utilization of a carrier system with polymer of similar backbone structure such as polycaprolactam [15].

Polyamide is a largely utilized polymer in textiles owing to its good mechanical and thermal properties, chemical stability, and biocompatibility. Polyamide is easily spinnable into homogeneous uniform nanofibers which are biocompatible but non-degradable which allows application of permanent nature and encourages reusability. Therefore, the polymer is commonly found in medical and protective textiles [25,26]. Despite the desirable properties and increasing use in medical textiles, a drawback associated with polyamide nanofibers is that it is a suitable carrier for bacterial growth. The drawback can be addressed through incorporation of antimicrobial agent and morphological manipulation avoiding non-homogeneous thick nanofibers [26–28].

Polyamide-6 (PA), also known as polycaprolactam, is formed by ring-opening polymerization of hexamethylenediamine. The polymer has a chemical structure of $(C_6H_{11}NO)_n$, with the lactam monomers held together by amide linkages. On the other hand, PL has a similar main backbone structure to PA with the additional cationic amino side chains [29,30]. Thus, a combination of PL with PA can be expected to result in spinnable fibers having a backbone of PA with the added cationic alpha-amino group providing antimicrobial function [15]. PL has an inherent antimicrobial function, is hydrophilic, and has low solution viscosity [15]. Thus, the incorporation of PL to PA nanofibers, along with incorporating antimicrobial function, is hypothesized to improve the characteristics of PA by forming uniform nanofibers with enhanced hydrophilicity. The non-toxic antimicrobial function will address the tendency of PA to be a carrier of bacterial growth [26–28]. Further, the improved hydrophilicity of PA can enhance user comfort while benefiting several forms of end-use, including the inner filter of a mask system, wound dressing, and sanitation [9,31,32]. The study thus explores a simple scalable method of obtaining PL nanofibers by utilizing the structurally similar PA as the base. Also, the study aims to enhance the utilization of PA polymer in medical and protective textiles, by addressing its drawbacks of bacterial growth and user discomfort.

2. Materials and Methods

2.1. Materials

Polyamide-6 (PA) (Mw = ~10,000 Da) and formic acid (88%, Macron Fine Chemicals) were purchased from Sigma-Aldrich (St. Louis, MO, USA). PL (Mw = ~ 3500-4700 Da) was purchased from Zhengzhou Bainafo Bioengineering Co., Ltd. (Henan, China). Escherichia coli K–12 bacterial culture and Nutrient Agar was purchased from Carolina Biological Supply Company (Burlington, NC, USA).

2.2. Preparation of Electrospinning Solution

Spinning solution was prepared by dissolving PA along with varying concentrations of PL in formic acid (88% concentration) under constant stirring overnight with a Burrell wrist-action® shaker, model-75 (Burrell Scientific LLC, Pittsburgh, PA, USA), to obtain a homogeneous solution. Formic acid was chosen as it allows environmentally friendly process over other toxic solvents like dimethylformamide (DMF).   Also, smooth PA fibers are expected with the organic solvent formic acid in comparison with other solvents like m-cresol or sulphuric acid, even at low polymer concentration [25,33]. The spinning solution compositions and sample codes are described in Table.1.

Table 1. Spinning solution compositions.

Sample code	Polyamide-6 Concentration	ε-Poly-L-lysine Concentration
Control	30% *(w/v)* of formic acid	0
PA/PL1	30% *(w/v)* of formic acid	0.5% *(w/w)* of PA
PA/PL2	30% *(w/v)* of formic acid	1.33% *(w/w)* of PA
PA/PL3	30% *(w/v)* of formic acid	10% *(w/w)* of PA
PA/PL4	30% *(w/v)* of formic acid	25% *(w/w)* of PA
PA/PL5	30% *(w/v)* of formic acid	40% *(w/w)* of PA
PA/PL6	30% *(w/v)* of formic acid	65% *(w/w)* of PA
PA/PL7	15% *(w/v)* of formic acid	100% *(w/w)* of PA

2.3. Electrospinning

Nanofiber membranes were developed using a single-needle electrospinning setup. Solution was continuously fed at a fixed rate using a syringe pump (Harvard Apparatus, Holliston, MA, USA). The distance between needle tip and grounded collector was set and a fixed high voltage was applied to the needle tip by a DC power supply instrument (Gamma High Voltage Research, Ormond Beach, FL, USA). Table 2 specifies the spinning parameters used for all the compositions.

Table 2. Electrospinning parameters.

Sample	Feed Rate	Supply Voltage	Spinning Distance	Collection Time
Control and PA/PL1 to PA/PL6	1ml/hour	20KV	12cm	4 hours
PA/PL7_A	1ml/hour	18KV	12cm	4 hours
PA/PL7_B	1ml/hour	16KV	12cm	4 hours
PA/PL7_C	1ml/hour	16KV	14cm	4 hours

2.4. Morphological Analysis

Morphological analysis of the electro spun nanofibers for their diameter and surface features was performed using a field emission scanning electron microscope (FESEM) (FEI Quanta 250, ThermoFisher Scientific, Waltham, MA, USA). Test samples were kept in vacuum overnight to evaporate any residual solvent prior to imaging. Image J software (National Institute of Health, Bethesda, MD, USA) was used to determine the diameter of the nanofibers. The average diameters were determined by measuring diameters of 50 representative fibers.

2.5. Fourier Transform Infrared (FTIR) Spectroscopy

The functional groups and presence of PL in developed nanofiber membranes were determined using an FTIR spectrometer (Perkin-Elmer Frontier FTIR, USA). The FTIR spectra were obtained in the range of 500–4000 cm^{-1} with 4 cm^{-1} wavenumber resolution, and each measurement consisted of 32 scans.

2.6. Water Contact Angle

The static water contact angle was measured as per ASTM-D7334-08 sessile drop method. The testing was conducted using a video-based drop shape analyzer (OCA 25, Data Physics GmbH, Regensburg, Germany) and the contact angles were measured with the built-in SCA20 software (V.4.5.20). For each sample, the contact angle measurement was repeated five times on separate membranes, and an average of the readings is reported.

2.7. Water Absorption Test

The water absorption capacity was measured through swelling ratio. The initial dry weight of 1cm*1cm sample was calculated (w1). Samples were then submerged in excess distilled water for 24 hours, followed by the measurement of their swollen weights (w2). The swelling ratio of each sample was then calculated in triplicate on separate membranes using the following equation 1 [34,35].

$$\text{Swelling ratio (g/g)} = \frac{w2 - w1}{w1} \tag{1}$$

2.8. Thermal Analysis

Thermal analysis was conducted using a differential scanning calorimeter (PerkinElmer DSC 4000, USA). Each sample (approximately 10 mg) was heated to 400 °C at a heating rate of 20 °C min^{-1}.

2.9. Mechanical Analysis

The tensile properties of the samples were tested as per ASTM-D882-09 using an Instron 5966 (Instron, Boston, MA, USA) tensile testing machine. The samples were tested with a load cell of 250 N, with 4cm between the clamps, and at a stretching rate set at 5 mm min^{-1}. Test specimens were prepared in dimensions 4 x1 inches and were conditioned at ambient conditions for a day prior to the testing. Testing was conducted on three separate membranes, for each sample, and an average of three readings is reported.

2.10. Antimicrobial Analysis

The antimicrobial testing was performed as per AATCC-147 zone inhibition method. Each sample was cut into circles of 1 cm diameter. Nutrient Agar plates were prepared and seeded with 1mL E.coli inoculums containing approximately 3x106 Colony Forming Units (CFU)/ml. The samples were placed on the plates and incubated for 24 hours at 37℃. Bacterial growth post-incubation for each sample was observed. Testing was conducted in triplicate on separate membranes for each composition.

2.11. Long Term Stability of Antimicrobial Property

To understand the ideal shelf life of the developed nanomembrane, the antimicrobial function was analyzed following AATCC-147 as described above at different time intervals (1 and 6 months) in triplicate. In between the testing, the nanofiber membranes were stored in plastic bags at room temperature.

2.12. Statistical Analysis

In this study, the results were analyzed using SPSS software (version 29.0; IBM Corp., Armonk, NY) using one-way analysis of variance (ANOVA) and Tukey statistical tests. All results are expressed as mean ± standard deviation and P-value < 0.05 was considered significant.

3. Results

3.1. Electrospinning of PA/PL Nanofiber Membranes

Solution properties and spinning parameters are crucial for successful execution of the electrospinning process. A delicate balance between the influential parameters is required to obtain smooth uniform nanofibers. For the successful spinning of PA into smooth uniform nanofibers, spinning parameters were set for the control sample (see Table 2). The parameters were further adjusted to ensure spinnability with increasing concentration of PL. Compositions PA/PL1 to PA/PL5 resulted in defect free nanofibers, thus validating the spinning parameters used for control sample. While PA/PA6 resulted in a flat nanoribbon structure with nonuniform diameter distribution (see Figure 1). Nanoribbon structure from this composition could be a result of increased viscosity due to the large amount of PL addition resulting in high polymer content in the system. The increased spinning solution viscosity results in thick jets during electrospinning. The dissipation of solvent during the jet's flight from spinneret to the collector is compromised due to the jet's excessive thickness. The dissipation of solvent molecules from jet core becomes difficult, resulting in a polymer skin on jet surface. Such jet collapses upon reaching the collector due to the solvent-rich interior forming the nanoribbon structure [2,36,37]. Thus, PA/PL5 was considered to be the maximum possible concentration of PL that can be added to the control spinning solution for set spinning parameters.

Further increment of PL required reduction in the base polymer concentration. Thus, for PA/PL7, the concentration of PA was reduced to 15% (w/v of formic acid) from the original 30% (w/v of formic acid). PA/PL7 was spun with varying parameters to determine suitable spinning parameters for the reduced PA and increased PL concentration. The voltage applied in electrospinning should be consistent with the viscosity, to ensure enough repulsive forces to overcome the surface tension of solution for the formation of Taylor's cone. Excessively high voltage can result in defects due to high jet instability and velocity [2,38,39]. The reduced base polymer content in the sample PA/PL7 is expected to reduce solution viscosity. Thus, PA/PL7_A was spun at reduced voltage of 18KV from the original 20KV voltage. Despite the reduced voltage, unspun beads were observed during the morphological analysis of PA/PL7_A (see Figure 1). The unspun beads could be a result of jet breakage due to high jet velocity facilitated by excess voltage. Thus, further decrement in voltage to 16KV was applied to PA/PL7_B and PA/PL7_C. Along with decreasing voltage, the spinning distance was increased in PA/PL7_C as beads could also arise from insufficient stretching of jet. The decreased voltage in PA/PL7_B resulted in nanofibers, however a few fibers exhibited flat ribbon like morphology. While the combination of decreased voltage with increased spinning distance in PA/PL7_C facilitated increased nanoribbon morphology (see Figure 1). The nanoribbon structure could be attributed to the decreased voltage ejecting thick jets. The thick jets during the flight time develop outer polymer skin and solvent-rich interior, which collapses into ribbon morphology. The increased distance seemed to facilitate the ribbon morphology due to the increased flight time assisting the outer layer of the thick jet to solidify, thus preventing the dissipation of solvent from the core [36]. Overall, the PA/PL7 series resulted in poor yield owing to the reduced base polymer concentration.
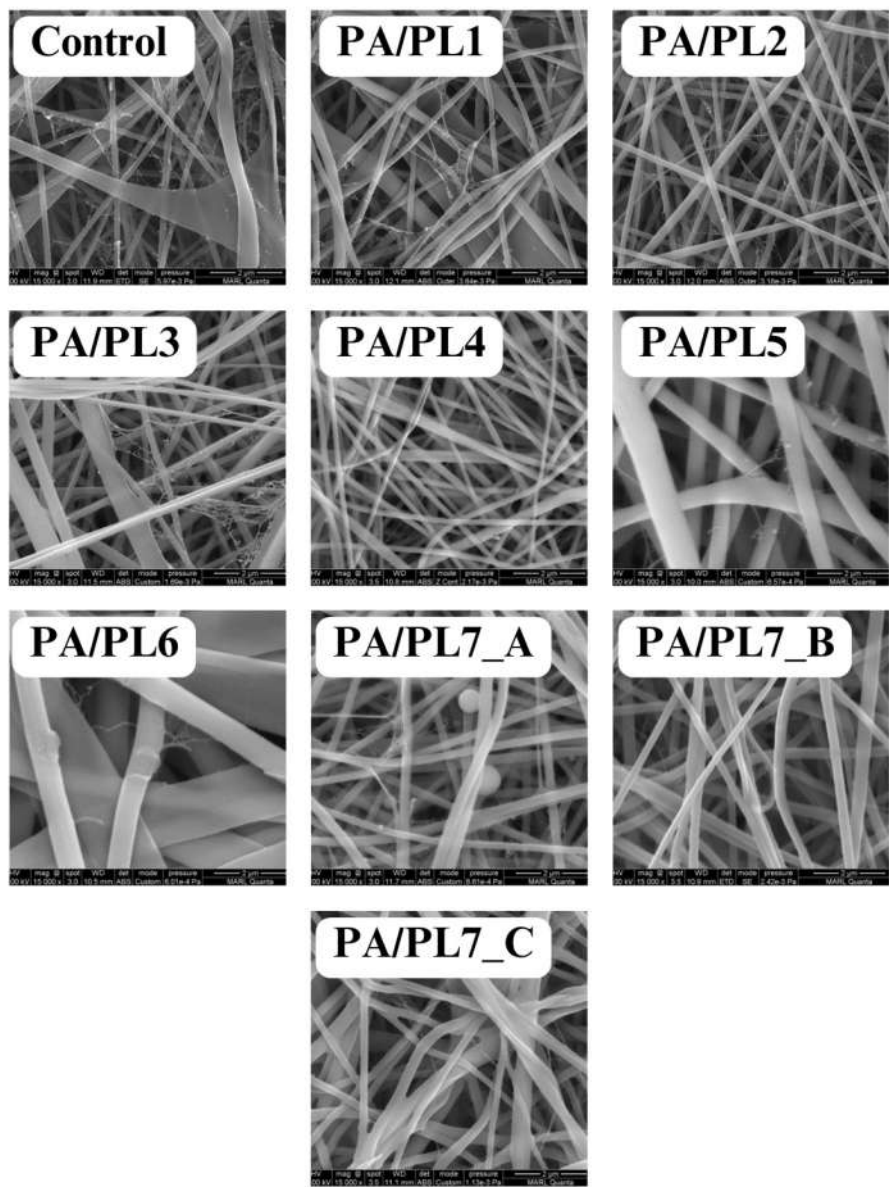
Figure 1. FESEM images of nanofiber membranes at 15000x.

3.2. Morphological Analysis

The effect of PL addition on morphology and diameter of nanofibers was analyzed using FESEM (see Figure 1). Table 3 summarizes the effect of PL addition on the diameter of the nanofibers. Figure 2 shows the fiber diameter distribution for each sample. A trend observed was a decrease in diameter from the control sample for PA/PL1 to PA/PL4. PL is of polycationic nature and has hydration capacity, resulting in reduced spinning solution viscosity and increased conductivity. This allows greater stretching of the spinning jet during electrospinning, thus explaining the thinner nanofibers [18,40,41]. Although PL addition to base PA polymer reduced the diameter of nanofibers, addition of PL beyond a certain amount, in this case PA/PL5 and further, increases the diameter. This is due to the increased polymer content for the ratio of solvent resulting in increased solution viscosity which in turn produces thicker jets during electrospinning. While most of the compositions (PA/PL1 to PA/PL5) resulted in defect-free continuous nanofibers. Defects were observed for certain compositions, beads for PA/PL7_A, flat ribbons morphology for PA/PL6 and PA/PL7_C, and overall poor yields for the PA/PL7 series. The reasoning behind the defects associated with respective composition is elaborated in the previous section. Lastly, nanoweb structures were observed in all the membranes. The formations of spider-net structure between polyamide nanofibers upon use of

formic acid as solvent is because of interaction between the amide group of PA and ionic species in formic acid [25]. These structures are expected to improve applicability in areas such as filtration.

Based on the morphological analysis, compositions with poor yield, nanoribbon structures, and nanofiber membranes with beads were excluded from further testing. Thus, the test samples for further characterization constitute defect-free homogenous nanofibers, namely, control; PA/PL1; PA/PL2; PA/PL3; PA/PL4; and PA/PL5.

Table 3. Average diameter of nanofibers.

Sample code	Diameter (Microns)
Control	0.22 ± 0.14 [ab]
PA/PL1	0.18 ± 0.10 [ab]
PA/PL2	0.16 ± 0.05 [b]
PA/PL3	0.18 ± 0.05 [ab]
PA/PL4	0.21 ± 0.05 [ab]
PA/PL5	0.43 ± 0.07 [c]
PA/PL6	1.06 ± 0.50 [d]
PA/PL7_A	0.24 ± 0.05 [ab]
PA/PL7_B	0.26 ± 0.07 [ab]
PA/PL7_C	0.28 ± 0.12 [a]

Different letters in the superscripts indicate significant difference ($p < 0.05$).
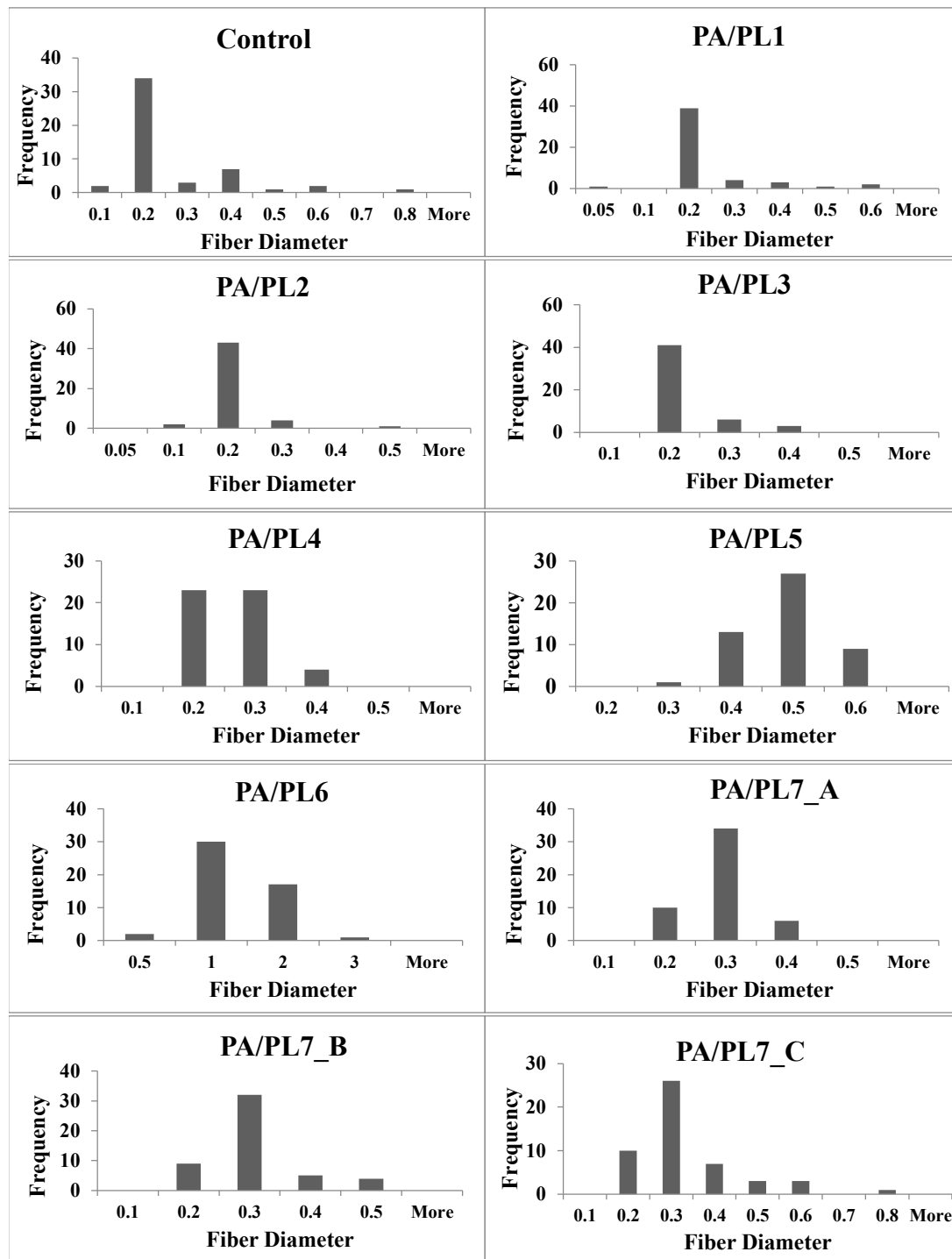
Figure 2. Fiber diameter distribution.

3.3. Fourier Transform Infrared (FTIR) Spectroscopy

The FTIR analysis demonstrated characteristic peaks of both PL and PA, confirming their presence in the nanofiber membranes (see Figure 3). Samples exhibited characteristic bands of PL with peaks at 1661 cm^{-1} and 1555 cm^{-1} indicating C=O and N-H_2 stretching vibration, respectively [17,18]. These peaks indicate the presence of PL. The absorption intensity of characteristic peaks of PL became stronger with increasing concentration of PL, indicating successful incorporation of high concentration of PL in the system [42]. Peaks observed at ~3300 cm^{-1} can be attributed to hydrogen-bonded N-H or O-H stretching vibration. The absorption intensity of these peaks also became stronger with increasing concentration of PL in the base PA, suggesting hydrogen bonding between

the polymer chains during electrospinning [43]. Additionally, all the PA/PL samples exhibited peaks at ~2900 cm^{-1} and 2935 cm^{-1}. These peaks signify C-H_2 stretching of polyamide [44]. Therefore, the FTIR analysis indicates the successful incorporation of PL to base PA and exhibits possibility of interaction between the polymers.
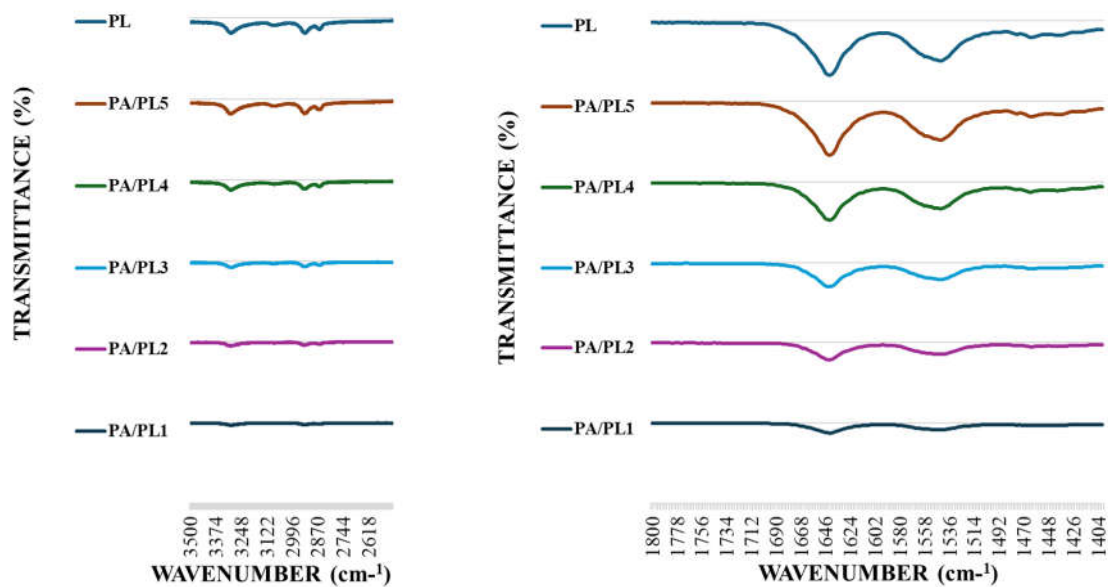

Figure 3. FTIR Spectroscopy of PL and PA/PL nanofiber membranes.

3.4. Analysis of Hydrophilic Behavior

3.4.1. Water Contact Angle

Static water contact angles of the samples were measured through sessile-drop method using a video-based drop shape analyzer. As seen in Table 4 and Figure 4, the contact angle significantly decreases with addition of PL. The decreased contact angle indicates improved hydrophilicity. The contact angles for the compositions PA/PL3, PA/PL4, and PA/PL5 were zero within the first 10 seconds of testing, indicating highly hydrophilic behavior. The improved hydrophilicity upon PL addition can be accounted for its inherent hydrophilic nature due to the large amino and amido groups [17,19,32].

Table 4. Hydration and mechanical properties of nanofiber membranes.

Sample code	Average Static Water Contact Angle	Average Swelling Ratio (g/g)	Tensile Strength (MPa)	Elongation (%)
Control	82.58 ± 9.75[a]	7.63 ± 3.98[a]	0.36 ± 0.03[a]	3.00 ± 0.84[a]
PA/PL1	40.37 ± 1.59 [b]	13.92 ± 2.79[ab]	0.33 ± 0.21[a]	7.83 ± 3.85 [b]
PA/PL2	18.25 ± 4.02 [c]	13.87 ± 0.61[ab]	0.53 ± 0.05 [a]	6.46 ± 1.19 [ab]
PA/PL3	0 [d]	14.86 ± 1.75[ab]	0.72 ± 0.26 [ab]	5.60 ± 1.01 [ab]
PA/PL4	0 [d]	15.20 ± 1.69[ab]	0.75 ± 0.19 [ab]	5.13 ± 0.40 [ab]
PA/PL5	0 [d]	18.10 ± 2.29[b]	1.02 ± 0.25 [b]	2.33 ± 0.50 [a]

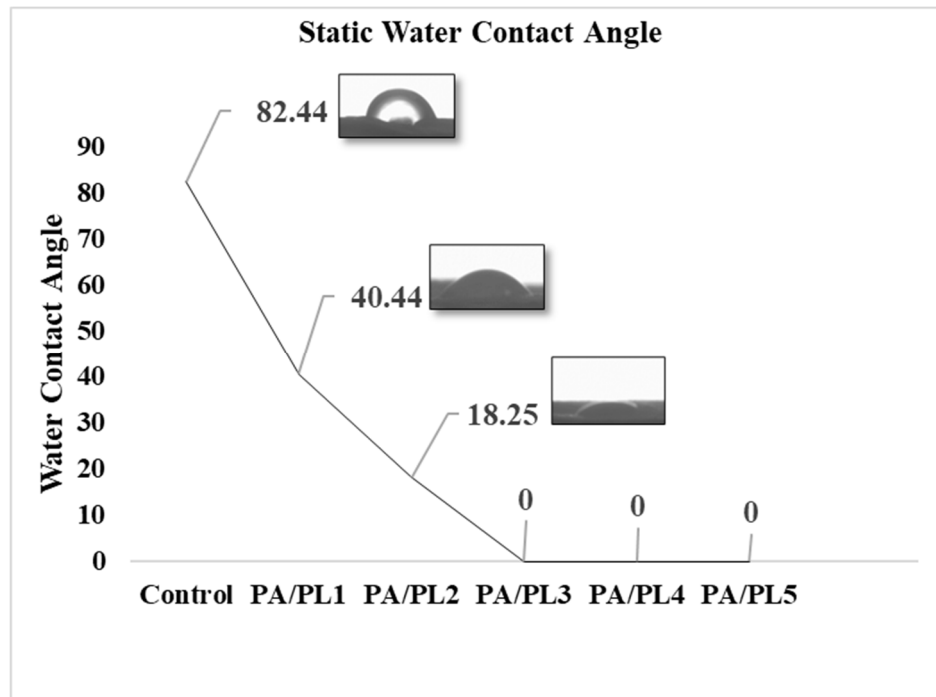Different letters in the superscripts indicate significant difference (p < 0.05).

Figure 4. Static water contact angle of nanofiber membranes.

3.4.2. Water Absorption Test

The hydrophilic behavior of samples was further analyzed through water absorption capacity by measuring the swelling ratio (see Table 4 and Figure 5). The swelling ratio of samples increased with PL concentration, with a significant increase for PA/PL5 from the control sample. Increased swelling ratio indicates better water uptake capacity through available hydrophilic sites [34,35]. These results are in alignment with the water contact angle results; therefore, it can be said that hydrophilicity of samples improved with increase in PL concentration owing to its inherent hydrophilic tendency [17,19,32].
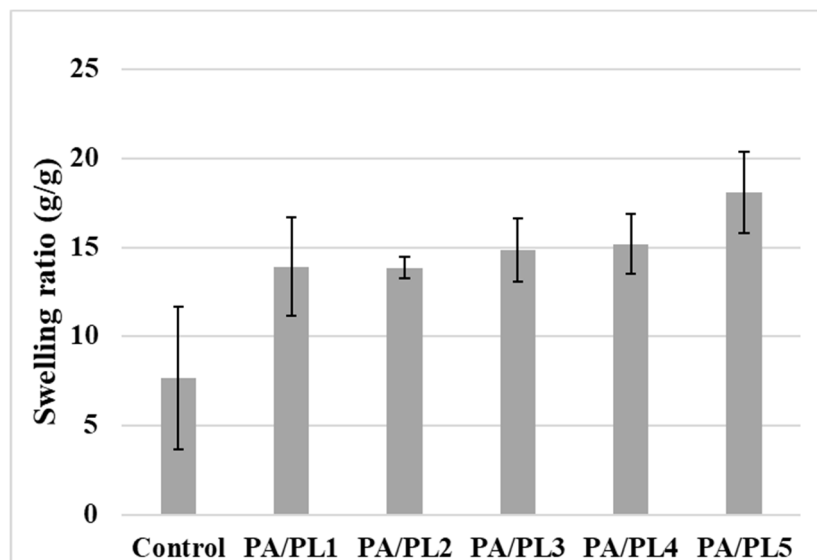

Figure 5. Average swelling ratio of nanofiber membranes.

3.5. Thermal Analysis

The thermal analysis of nanofiber membranes are shown in Figure 6. Endothermic peaks were observed for all the samples representing the melting behavior of the nanofiber membranes. The

thermal analysis of PA/PL3, PA/PL4, and PA/PL5 samples showcased multiple melting peaks indicating secondary crystallization (melting – recrystallization – remelting) [45,46]. The onset of melting for control, PA/PL1, PA/PL2, PA/PL3, PA/PL4, and PA/PL 5 was at 207.05°C, 207.54°C, 207.01°C, 207.78°C, 208.17°C, and 208.3°C, respectively. The improved thermal stability of the nanofiber membranes upon addition of PL indicates no disruption to PA structure and possible interaction between PA and PL polymers [18].
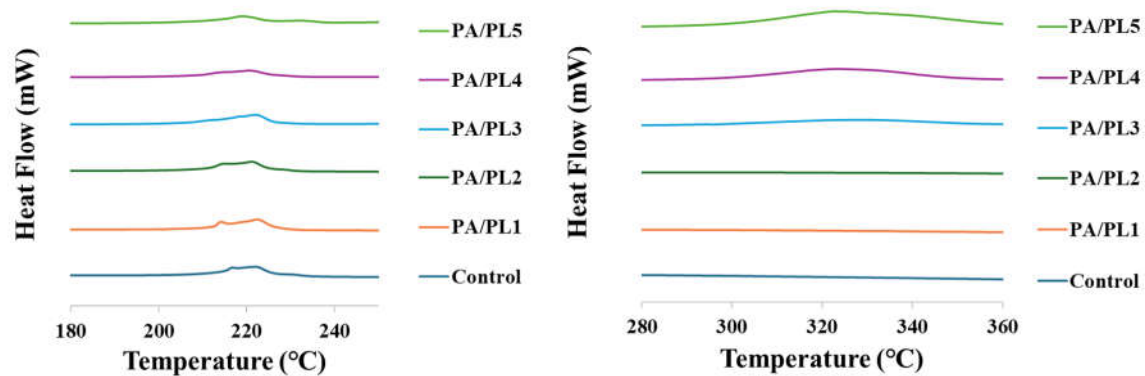

Figure 6. Differential scanning calorimetry curve of nanofiber membranes.

3.6. Mechanical Analysis

The mechanical properties of the samples in terms of tensile strength and elongation are summarized in Table 4. The addition of PL indicated an increasing trend in tensile strength of PA, with a significant increase for PA/PL5 from the control sample. The increasing tensile strength is an indication of no disruption to PA structure after addition of PL, along with possible interaction between the polymers [47]. The increasing tensile strength could be tied to the FTIR analysis suggesting hydrogen bonding upon addition of PL, as introduction of amino and amide bonds to peptide chain provides more hydrogen bonding [43]. Further, the improved thermal stability with increasing concentration of PL as shown in thermal analysis also indicates interaction between the two polymers [18]. As for the elongation, initial PL concentrations indicated an increasing trend in the elongation %. However, as expected the increase in elongation declined for higher PL concentration. The reduced elongation % with increased tensile strength can be tied to the increased rigidity and crystallinity as a result of interactions between PA and PL. However, the elongation % did not have a significant deterioration from the control sample.

3.7. Antimicrobial Analysis

Antimicrobial activity of the developed compositions was tested through zone inhibition testing. The testing demonstrates antimicrobial function of test sample upon observation of inhibition zone surrounding the sample when plated with test bacteria [48]. Figure 7 is a representative image of the testing. Zones of inhibition were seen for the samples PA/PL4, and PA/PL5 indicating antimicrobial activity against the tested bacteria E.coli, with highest antimicrobial activity for PA/PL5 (see Figure 8). PL has inherent cationic antimicrobial function owing to the α-amino side group [12,14,15]. The FTIR analysis confirmed the presence of PL and cationic amino group in the samples, which are responsible for inducing antimicrobial activity to base PA. The antimicrobial testing's disclosed that base PA consisting of 40% (w/w) PL of PA is successful in establishing efficient antimicrobial function. Addition of PL in concentrations lower than 25% (w/w) of PA did not exhibit an inhibition zone thus being insufficient to induce antimicrobial function to the base PA. The efficient antimicrobial activity of PA/PL5 could be tied to high concentration of PL and defect-free homogeneous morphology.
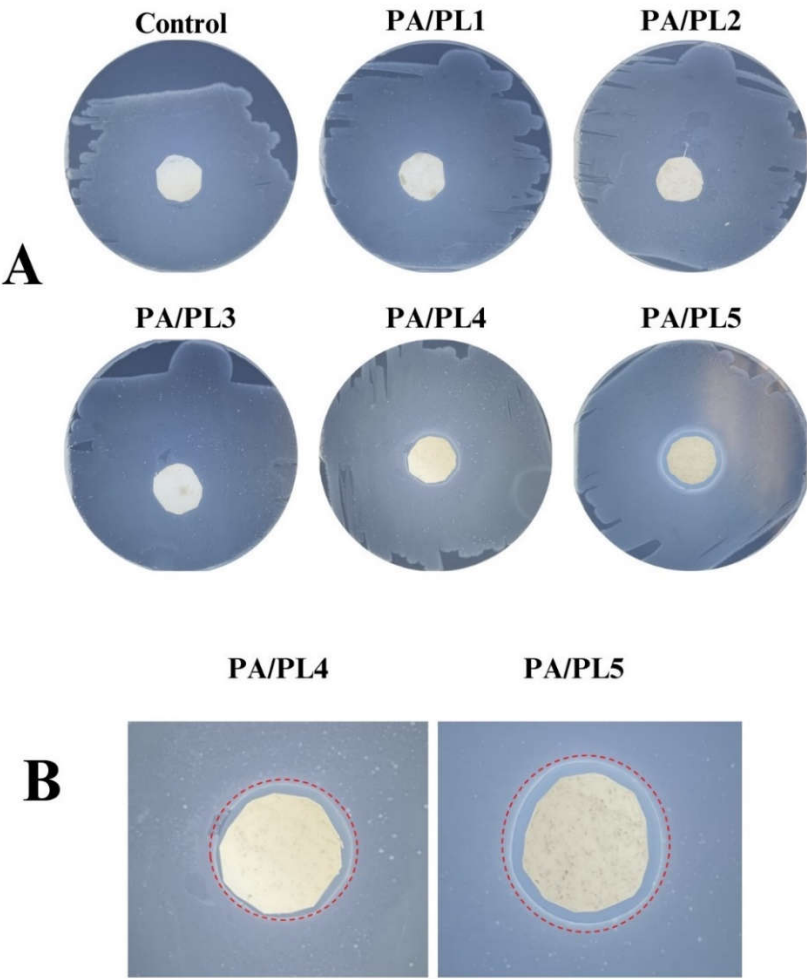
Figure 7. A) Antimicrobial activity of the nanofiber membranes and B) Zoomed-in views of the observed zones of inhibition.
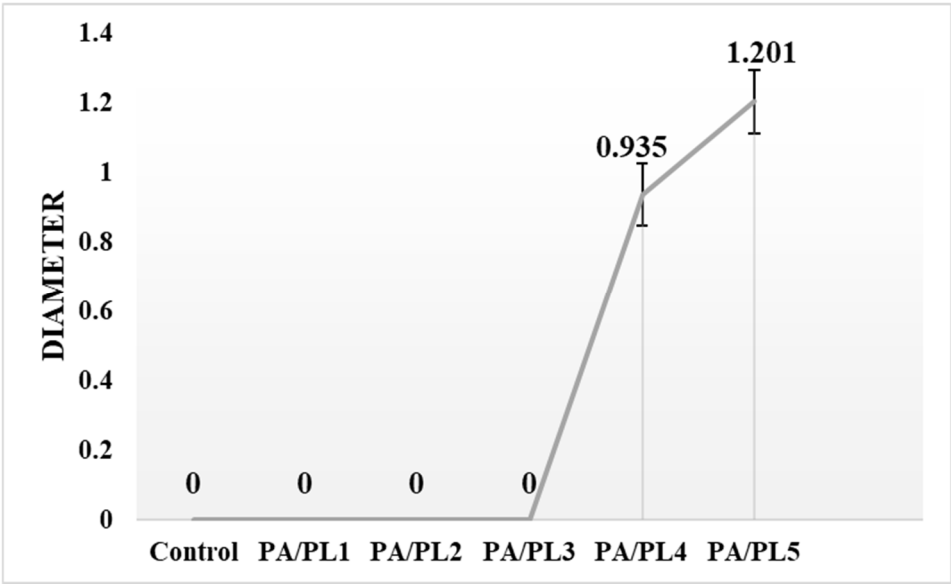
Figure 8. Average areas of antimicrobial zones of inhibition for all the nanofiber membranes.

3.8. Long-Term Stability of Antimicrobial Property

The characterization of antimicrobial agent in textile can be versatile, addressing aspects crucial to intended applications, such as storage, reusability, or long-term stability [9,49,50]. PL is a cationic polymer exhibiting antimicrobial function through the positively charged amino side groups. Although cationic polymers such as PL have an advantage of better stability over leaching antimicrobial agent, cationic polymers can still experience proliferation of bacteria on the surface once the surface is sufficiently covered with microorganisms due to the exhaustion of cations [7,23,24,49]. Thus, it is important to analyze the long-term stability of antimicrobial textiles. Despite the importance of this testing to be able to define an appropriate shelf-life ensuring functionality, its inclusion in antimicrobial characterization was found to be uncommon [26]. The long-term stability of

PA/PL 5 sample was characterized at 1 and 6 months. As seen in Figure 9, the antimicrobial activity through observed zone of inhibition remains to be effective till 6 months. This testing allows us to define the 6-month shelf life of developed PA/PL5 without any deterioration in antimicrobial activity.
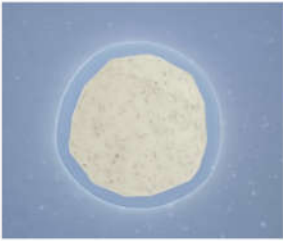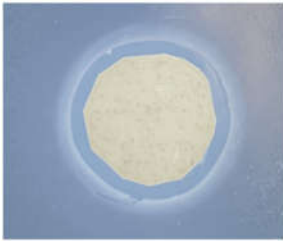

PA/PL5		
Timeline	1 month	6 month
Average zone inhibition area	1.20 ± 0.09	1.19 ± 0.18

Figure 9. Long-term stability of antimicrobial activity for PA/PL5.

4. Conclusions and Future Scope

PA is a popular polymer for functional textile applications due to its excellent mechanical and thermal properties, chemical stability, and biocompatibility. However, PA nanofibers tend to promote bacterial growth limiting its use in medical textiles. On the other hand, PL is a naturally occurring homopolyamide known for its non-toxicity, hydrophilicity, and antimicrobial properties, but its low molecular weight prevents its spinnability. Given the structural similarity between PL and PA with PL having additional amino side chain, this study addresses the spinnability of PL by utilizing PA as the carrier, while hypothesizing enhanced PA properties.

The study demonstrates spinnability of varying concentration of PL with base PA, including higher concentration of PL than previously reported. The effect of PL addition on morphology, hydrophilicity, thermal stability, mechanical property, and antimicrobial activity were thoroughly investigated. Among the various compositions developed and characterized, PA/PL5 was identified as the maximum spinnable concentration of PL that allowed enhanced properties in PA resulting in superhydrophilicity, improved thermal and mechanical behavior, and efficient antimicrobial property with long-term stability.

This study presents a simple scalable method to produce spinnable fibers with PA backbone and the added cationic α-amino group from PL. This method can enhance industrial utilization of PA in functional textiles by improving mechanical performance, improved hydrophilicity, and stable antimicrobial function. These findings suggest significant potential for specific applications, such as respiratory protection, wound dressing, and sanitation.

14

References

1. Zhang X. Fundamentals of fiber science. DEStech Publications, Inc; 2014 Jan 13.

2. Xue J, Wu T, Dai Y, Xia Y. Electrospinning and electrospun nanofibers: Methods, materials, and applications. Chemical reviews. 2019 Mar 27;119(8):5298-415. https://doi.org/10.1021/acs.chemrev.8b00593

3. Khan WS, Asmatulu R, Ceylan M, Jabbarnia A. Recent progress on conventional and non-conventional electrospinning processes. Fibers and Polymers. 2013 Aug;14:1235-47. https://doi.org/10.1007/s12221-013-1235-8

4. Li Y, Zhu J, Cheng H, Li G, Cho H, Jiang M, Gao Q, Zhang X. Developments of advanced electrospinning techniques: A critical review. Advanced Materials Technologies. 2021 Nov;6(11):2100410. https://doi.org/10.1002/admt.202100410

5. Gupta, D. (2011). Functional clothing-Definition and classification. Indian Journal of Fiber and Textile Research, 36, 321-326.   http://nopr.niscpr.res.in/handle/123456789/13225

6. Zhang, Y., Xia, X., Ma, K., Xia, G., Wu, M., Cheung, Y. H., ... & Xin, J. H. (2023). Functional Textiles with Smart Properties: Their Fabrications and Sustainable Applications. Advanced Functional Materials, 2301607. https://doi.org/10.1002/adfm.202301607

7. Riga EK, Vöhringer M, Widyaya VT, Lienkamp K. Polymer-based surfaces designed to reduce biofilm formation: from antimicrobial polymers to strategies for long-term applications. Macromolecular rapid communications. 2017 Oct;38(20):1700216. https://doi.org/10.1002/marc.201700216

8. Qiu H, Si Z, Luo Y, Feng P, Wu X, Hou W, Zhu Y, Chan-Park MB, Xu L, Huang D. The mechanisms and the applications of antibacterial polymers in surface modification on medical devices. Frontiers in bioengineering and biotechnology. 2020 Nov 11;8:910. https://doi.org/10.3389/fbioe.2020.00910

9. Stokes K, Peltrini R, Bracale U, Trombetta M, Pecchia L, Basoli F. Enhanced medical and community face masks with antimicrobial properties: A systematic review. Journal of Clinical Medicine. 2021 Sep 9;10(18):4066. https://doi.org/10.3390/jcm10184066

10. Bhandari V, Jose S, Badanayak P, Sankaran A, Anandan V. Antimicrobial finishing of metals, metal oxides, and metal composites on textiles: a systematic review. Industrial & Engineering Chemistry Research. 2022 Jan 2;61(1):86-101. https://doi.org/10.1021/acs.iecr.1c04203

11. Karypidis M, Karanikas E, Papadaki A, Andriotis EG. A Mini-Review of Synthetic Organic and Nanoparticle Antimicrobial Agents for Coatings in Textile Applications. Coatings. 2023 Mar 28;13(4):693. https://doi.org/10.3390/coatings13040693

12. Tao Y, Chen X, Jia F, Wang S, Xiao C, Cui F, Li Y, Bian Z, Chen X, Wang X. New chemosynthetic route to linear ε-poly-lysine. Chemical Science. 2015;6(11):6385-91.10.1039/C5SC02479J

13. Patil NA, Kandasubramanian B. Functionalized polylysine biomaterials for advanced medical applications: A review. European Polymer Journal. 2021 Mar 5;146:110248. https://doi.org/10.1016/j.eurpolymj.2020.110248

14. Shoji S, Hiroyoshi M, Toshiro I, Heiichi S. Antimicrobial action of ε-poly-l-lysine. The Japanese Journal of Antibiotics. 1984;37(11):1449-55. https://doi.org/10.7164/antibiotics.37.1449

15. Li M, Tao Y. Poly (ε-lysine) and its derivatives via ring-opening polymerization of biorenewable cyclic lysine. Polymer Chemistry. 2021;12(10):1415-24.10.1039/D0PY01387K

16. Lin L, Xue L, Duraiarasan S, Haiying C. Preparation of ε-polylysine/chitosan nanofibers for food packaging against Salmonella on chicken. Food Packaging and Shelf Life. 2018 Sep 1;17:134-41. https://doi.org/10.1016/j.fpsl.2018.06.013

17. Wu C, Sun J, Lu Y, Wu T, Pang J, Hu Y. In situ self-assembly chitosan/ε-polylysine bionanocomposite film with enhanced antimicrobial properties for food packaging. International Journal of Biological Macromolecules. 2019 Jul 1;132:385-92. https://doi.org/10.1016/j.ijbiomac.2019.03.133

18. Liu F, Liu Y, Sun Z, Wang D, Wu H, Du L, Wang D. Preparation and antibacterial properties of ε-polylysine-containing gelatin/chitosan nanofiber films. International journal of biological macromolecules. 2020 Dec 1;164:3376-87. https://doi.org/10.1016/j.ijbiomac.2020.08.152

19. Mayandi V, Wen Choong AC, Dhand C, Lim FP, Aung TT, Sriram H, Dwivedi N, Periayah MH, Sridhar S, Fazil MH, Goh ET. Multifunctional antimicrobial nanofiber dressings containing ε-polylysine for the eradication of bacterial bioburden and promotion of wound healing in critically colonized wounds. ACS applied materials & interfaces. 2020 Mar 16;12(14):15989-6005. https://doi.org/10.1021/acsami.9b21683

20. Dias YJ, Robles JR, Sinha-Ray S, Abiade J, Pourdeyhimi B, Niemczyk-Soczynska B, Kolbuk D, Sajkiewicz P, Yarin AL. Solution-blown poly (hydroxybutyrate) and ε-poly-l-lysine submicro-and microfiber-based sustainable nonwovens with antimicrobial activity for single-use applications. ACS Biomaterials Science & Engineering. 2021 Jul 26;7(8):3980-92. https://doi.org/10.1021/acsbiomaterials.1c00594

21. Zhang, X., Shi, C., Liu, Z., Pan, F., Meng, R., Bu, X., ... & Yu, L. (2018). Antibacterial activity and mode of action of ε-polylysine against Escherichia coli O157: H7. Journal of Medical Microbiology, 67(6), 838-845.

22. Wahid F, Wang FP, Xie YY, Chu LQ, Jia SR, Duan YX, Zhang L, Zhong C. Reusable ternary PVA films containing bacterial cellulose fibers and ε-polylysine with improved mechanical and antibacterial properties. Colloids and Surfaces B: Biointerfaces. 2019 Nov 1;183:110486. https://doi.org/10.1016/j.colsurfb.2019.110486

23. Banerjee, I., Pangule, R. C., & Kane, R. S. (2011). Antifouling coatings: recent developments in the design of surfaces that prevent fouling by proteins, bacteria, and marine organisms. Advanced materials, 23(6), 690-718.

24. Babutan, I., Lucaci, A. D., & Botiz, I. (2021). Antimicrobial polymeric structures assembled on surfaces. Polymers, 13(10), 1552.

25. Matulevicius J, Kliucininkas L, Martuzevicius D, Krugly E, Tichonovas M, Baltrusaitis J. Design and characterization of electrospun polyamide nanofiber media for air filtration applications. Journal of nanomaterials. 2014 Jan 1;2014:14-14.

26. Lencova S, Zdenkova K, Jencova V, Demnerova K, Zemanova K, Kolackova R, Hozdova K, Stiborova H. Benefits of polyamide nanofibrous materials: Antibacterial activity and retention ability for Staphylococcus aureus. Nanomaterials. 2021 Feb 13;11(2):480. https://doi.org/10.3390/nano11020480

27. Lencova S, Svarcova V, Stiborova H, Demnerova K, Jencova V, Hozdova K, Zdenkova K. Bacterial biofilms on polyamide nanofibers: factors influencing biofilm formation and evaluation. ACS applied materials & interfaces. 2020 Dec 7;13(2):2277-88. https://doi.org/10.1021/acsami.0c19016

28. Lencova S, Stiborova H, Munzarova M, Demnerova K, Zdenkova K. Potential of Polyamide Nanofibers With Natamycin, Rosemary Extract, and Green Tea Extract in Active Food Packaging Development: Interactions With Food Pathogens and Assessment of Microbial Risks Elimination. Frontiers in Microbiology. 2022 Mar 15;13:857423. https://doi.org/10.3389/fmicb.2022.857423

29. Ushimaru K, Hamano Y, Katano H. Antimicrobial activity of ε-poly-L-lysine after forming a water-insoluble complex with an anionic surfactant. Biomacromolecules. 2017 Apr 10;18(4):1387-92. https://doi.org/10.1021/acs.biomac.7b00109

30. Ushimaru K, Morita T, Fukuoka T. Bio-based, flexible, and tough material derived from ε-Poly-l-lysine and fructose via the maillard reaction. ACS omega. 2020 Aug 31;5(36):22793-9. https://doi.org/10.1021/acsomega.0c01813

31. Songer J. Adopting Who Guidance on Fabric Masks for COVID-19. Available at SSRN 3632531. 2020 Jun 22.

32. Zhang W, Li JX, Tang RC, Zhai AD. Hydrophilic and antibacterial surface functionalization of polyamide fabric by coating with polylysine biomolecule. Progress in Organic Coatings. 2020 May1; 142:105571. https://doi.org/10.1016/j.porgcoat.2020.105571

33. Ojha SS, Afshari M, Kotek R, Gorga RE. Morphology of electrospun nylon-6 nanofibers as a function of molecular weight and processing parameters. Journal of applied polymer science. 2008 Apr 5;108(1):308-19. https://doi.org/10.1002/app.27655

34. Almasian A, Giahi M, Fard GC, Dehdast SA, Maleknia L. Removal of heavy metal ions by modified PAN/PANI-nylon core-shell nanofibers membrane: Filtration performance, antifouling and regeneration behavior. Chemical Engineering Journal. 2018 Nov 1;351:1166-78.

35. Cay A, Miraftab M. Properties of electrospun poly (vinyl alcohol) hydrogel nanofibers crosslinked with 1, 2, 3, 4-butanetetracarboxylic acid. Journal of applied polymer science. 2013 Sep 15;129(6):3140-9.

36. Koombhongse S, Liu W, Reneker DH. Flat polymer ribbons and other shapes by electrospinning. Journal of Polymer Science Part B: Polymer Physics. 2001 Nov 1;39(21):2598-606. https://doi.org/10.1002/polb.10015

37. Itoh H, Li Y, Chan KH, Kotaki M. Morphology and mechanical properties of PVA nanofibers spun by free surface electrospinning. Polymer Bulletin. 2016 Oct;73:2761-77. https://doi.org/10.1007/s00289-016-1620-8

38. Şener AG, Altay AS, Altay F. Effect of voltage on morphology of electrospun nanofibers. In2011 7th International Conference on Electrical and Electronics Engineering (ELECO) 2011 Dec 1 (pp. I-324). IEEE.

39. Haider A, Haider S, Kang IK. A comprehensive review summarizing the effect of electrospinning parameters and potential applications of nanofibers in biomedical and biotechnology. Arabian Journal of Chemistry. 2018 Dec 1;11(8):1165-88. https://doi.org/10.1016/j.arabjc.2015.11.015

40. Han Y, Shi C, Cui F, Chen Q, Tao Y, Li Y. Solution properties and electrospinning of polyacrylamide and ε-polylysine complexes. Polymer. 2020 Sep 9;204:122806. https://doi.org/10.1016/j.polymer.2020.122806

41. Bhardwaj N, Kundu SC. Electrospinning: A fascinating fiber fabrication technique. Biotechnology advances. 2010 May 1;28(3):325-47. https://doi.org/10.1016/j.biotechadv.2010.01.004

42. Hsu CP. Infrared spectroscopy. Handbook of instrumental techniques for analytical chemistry. 1997 Jun 14;249.

43. Zhang S, Chen H, Shi Z, Liu Y, Liu L, Yu J, Fan Y. Preparation of amino cellulose nanofiber via ε-poly-L-lysine grafting with enhanced mechanical, anti-microbial and food preservation performance. Industrial Crops and Products. 2023 Apr 1;194:116288.

44. Rotter G, Ishida H. FTIR separation of nylon-6 chain conformations: Clarification of the mesomorphous and γ-crystalline phases. Journal of Polymer Science Part B: Polymer Physics. 1992 Apr;30(5):489-95. https://doi.org/10.1002/polb.1992.090300508

45. Gunaratne LM, Shanks RA. Multiple melting behaviour of poly (3-hydroxybutyrate-co-hydroxyvalerate) using step-scan DSC. European Polymer Journal. 2005 Dec 1;41(12):2980-8.

46. Asran AS, Razghandi K, Aggarwal N, Michler GH, Groth T. Nanofibers from blends of polyvinyl alcohol and polyhydroxy butyrate as potential scaffold material for tissue engineering of skin. Biomacromolecules. 2010 Dec 13;11(12):3413-21.

47. Han Y, Xu Y, Zhang S, Li T, Ramakrishna S, Liu Y. Progress of improving mechanical strength of electrospun nanofibrous membranes. Macromolecular Materials and Engineering. 2020 Nov;305(11):2000230. https://doi.org/10.1002/mame.202000230

48. Pinho E, Magalhães L, Henriques M, Oliveira R. Antimicrobial activity assessment of textiles: standard methods comparison. Annals of microbiology. 2011 Sep;61:493-8. https://doi.org/10.1007/s13213-010-0163-8

49. Tofail SA, Bauer J. Electrically Mediated Interactions at the Materials/Biology Interface. InElectrically Active Materials for Medical Devices 2016 (pp. 1-18). https://doi.org/10.1142/9781783269877_0001

50. Monticello RA, Askew PD. Antimicrobial textiles and testing techniques. Russell, Hugo & Ayliffe's: Principles and Practice of Disinfection, Preservation and Sterilization. 2013 Jan 10:520-9. https://doi.org/10.1002/9781118425831.ch20d